Catalytic reduction of N_2O by CO over $Pt_lAu_m^-$ clusters: A first-principles study

Mi Hong(米 鸿)[a], Wei Shi-Hao(韦世豪)[a,†], Duan Xiang-Mei(段香梅)[b], and Pan Xiao-Yin(潘孝胤)[b]

[a] *Department of Microelectronic Science and Engineering, Faculty of Science, Ningbo University, Ningbo* 315211, *China*
[b] *Department of Physics, Faculty of Science, Ningbo University, Ningbo* 315211, *China*

(Received 8 April 2015; revised manuscript received 27 May 2015; published online 20 July 2015)

Based on the density functional theory, we investigate negatively charged clusters $Pt_lAu_m^-$ $(l+m=4)$, which show significant catalytic properties in the simultaneous removal of N_2O and CO. We find that in these clusters, the platinum atom acts as the adsorption center for N_2O, the gold and Pt atoms act as electron donors during the reaction, and the charge transfers from the bimetallic cluster to the N_2O molecule. As the proportion of Au in the cluster increases, the d band center shifts down further away from the Fermi level, meanwhile more charge is transferred to the N_2O molecule, resulting in weaker N–O bond strength. Therefore bimetallic cluster $PtAu_3^-$ shows better catalytic properties than the other clusters, especially pure Pt_4^- and Au_4^- clusters. This means that there is a synergetic effect between the Pt and Au atoms in the negatively charged bimetallic clusters. Our results help to reveal the mechanism of $Pt_lAu_m^-$ bimetallic clusters as excellent catalysts.

Keywords: bimetallic cluster, translate state, catalytic property, potential energy surface

PACS: 82.33.Hk, 36.40.Cg, 31.15.Ve **DOI:** 10.1088/1674-1056/24/9/098201

1. Introduction

Nitrous oxide (N_2O), as a production from the combustion of fossil fuels, has been recognized as one of the contributors to global warming, and its global warming potential (GWP) is 300 times greater than that of carbon dioxide (CO_2). N_2O can also cause ozone depletion.[1] As another main harmful component in the stack gases, CO not only always co-exists with N_2O in the combustion exhausts, but also is an excellent reducing gas. How to reduce the environmental pollution of N_2O has been a hot subject for many experimental and theoretical research studies.[2–9] The density functional theory (DFT) has been widely used to study the properties of molecules and materials, because DFT can reveal detailed mechanisms at atomic level for the cluster reactions.[10–12]

The platinum-based catalyst is one of the most efficient catalysts for numerous important reactions, such as oxidation of CO to CO_2.[13] The conversion of N_2O and CO to N_2 and CO_2 catalyzed by neutral platinum clusters and their charged counterparts have been investigated.[14–17] To the best of our knowledge, neutral platinum clusters and their positively charged counterparts are not active catalysts for the conversion of CO to CO_2 with N_2O. Fortunately, Siu *et al.* found that Pt_4^- is a very active catalyst for the conversion of CO to CO_2 with N_2O.[18] However, the pure platinum catalyst is very expensive. So promising alternatives with high activity and lower price are required. Recently, the platinum-based bimetallic clusters have attracted special attention for their novel properties and high catalytic activities. It is proposed that the platinum catalysts alloyed or modified by other metals, such as ruthenium, palladium, and gold could exhibit higher activity for CO oxidation. Among the platinum-based bimetallic catalysts, platinum-gold nanoparticles are of particular interest for their superior catalytic performance.[19–21] No study has been carried out involving the reduction of N_2O by CO over platinum-gold bimetallic catalysts.

In this paper, we perform a density functional theory (DFT) study to investigate the catalytic properties of four negatively charged clusters $Pt_lAu_m^-$ $(l+m=4)$ in the conversion of N_2O and CO to N_2 and CO_2. We find that with the increase of the proportion of gold atoms in the cluster, the catalytic properties can be dramatically enhanced, and as the percentage of platinum is reduced, the cost of the catalyst is greatly reduced.

2. Calculations

All calculations were carried out using the density functional theory with the generalized gradient approximation (GGA) and the revised Perdew, Burke, and Ernzerhof exchange–correlation (RPBE)[22] as implemented in the DMOL^3 computational software package.[23,24] The strong relativistic effect of Pt and Au has been considered. The spin polarization was included and no symmetric constraints were imposed in all calculations. In the self-consistent-field (SCF) calculation, the optimization convergence thresholds for en-

*Project supported by the National Natural Science Foundation of China (Grants Nos. 10804058, 11174164, and 11275100), the Science Foundation of Zhejiang Province, China (Grant No. Y607546), and the K. C. Wong Magna Foundation in Ningbo University, China.

†Corresponding author. E-mail: weishihao@nbu.edu.cn

© 2015 Chinese Physical Society and IOP Publishing Ltd

ergy change, maximum force, and maximum displacement were 2.0×10^{-5} Ha, 4.0×10^{-3} Ha/Å, and 5.0×10^{-3} Å, respectively.

The overall reduction of N_2O by CO can be written as

$$N_2O + CO \xrightarrow{\text{catalyst}} N_2 + CO_2. \quad (1)$$

It can be divided into two elementary reactions

$$N_2O \xrightarrow{\text{catalyst}} N_2 + O, \quad (2)$$

$$CO + O \xrightarrow{\text{catalyst}} CO_2. \quad (3)$$

The adsorption energy E_{ads} of N_2O to $Pt_lAu_m^-$ clusters is defined as

$$E_{\text{ads}} = -[E_{[Pt_lAu_m(N_2O)]^-} - E_{[Pt_lAu_m]^-} - E_{N_2O}], \quad (4)$$

where $E_{[Pt_lAu_m(N_2O)]^-}$ is the total energy of the absorption system, $E_{[Pt_lAu_m]^-}$ is the total energy of the $Pt_lAu_m^-$ clusters, and E_{N_2O} is the total energy of an isolated N_2O molecule.

The desorption energy $E_{\text{des}}^{\text{Mol}}$ of N_2 or CO_2 from the cluster can be obtained with the following equation:

$$E_{\text{des}}^{\text{Mol}} = -[E_{\text{Mol}\cdot(*)} - E_{(*)} - E_{\text{Mol}}], \quad (5)$$

where $E_{\text{Mol}\cdot(*)}$ is the total energy of the $[Pt_lAu_mO\cdot N_2]^-$ or $[Pt_lAu_m\cdot CO_2]^-$ cluster; $E_{(*)}$ is the total energy of the $[Pt_lAu_mO]^-$ or $[Pt_lAu_m]^-$ cluster; and E_{Mol} is the total energy of an isolated N_2 or CO_2 molecule.

The dissociation energy E_{dis} for the negatively charged $Pt_lAu_m^-$ clusters is defined as

$$E_{\text{dis}} = (l-1)E_{\text{Pt}} + mE_{\text{Au}} + E_{[\text{Pt}]^-} - E_{[Pt_lAu_m]^-}, \quad (6)$$

where E_{Pt}, E_{Au}, and $E_{[\text{Pt}]^-}$ are the total energies of the Pt, Au, and Pt^- atoms, respectively.

In order to analyze the catalytic activity of the $Pt_lAu_m^-$ clusters with different weights of Au, we use the average energy of the occupied M 5d band center (E_{d}), which is given by

$$E_{\text{d}} = \frac{\sum_{\varepsilon\to-\infty}^{E_{\text{F}}} \varepsilon n(\varepsilon)}{\sum_{\varepsilon\to-\infty}^{E_{\text{F}}} n(\varepsilon)}, \quad (7)$$

where E_{F} is the Fermi level, and $n(\varepsilon)$ is the Mulliken population of the energy level ε for M 5d orbitals. The occupied M 5d band center is marked by the black arrows in Fig. 3.

The activation energies for the above two elementary reactions are identified by complete linear synchronous transition and quadratic synchronous transit search methods, following by transition-state optimization and confirmation. The optimized transitional points on the potential energy surface are verified by the second-order derivatives of the energy with respect to the atomic coordinates (Hessian) through vibrational frequency calculations.

3. Results and discussion

3.1. Binding and dissociation of N_2O on $Pt_lAu_m^-$ cluster

In Table 1, we list the adsorption energy of N_2O (E_{ads}), the largest activate energies $E_{\text{a}}^{\text{max}}(N_2O)$ (for the elementary reaction $N_2O \rightarrow N_2 + O$) and $E_{\text{a}}^{\text{max}}(CO)$ (for the elementary reaction $CO + O \rightarrow CO_2$), and the desorption energies $E_{\text{des}}^{N_2}$ (for N_2) and $E_{\text{des}}^{CO_2}$ (for CO_2) in the reaction pathway of the $Pt_lAu_m^-$ clusters. The dissociation energy E_{dis} of the $Pt_lAu_m^-$ clusters is also listed (the value in the parenthesis is E_{dis} of the Pt_lAu_m clusters). We find that E_{dis} for the negatively charged $Pt_lAu_m^-$ clusters is larger than that for their neutral counterparts. At the same time, all E_{dis} for the $Pt_lAu_m^-$ clusters are larger than 2.00 eV. It means that the $Pt_lAu_m^-$ clusters are more stable than their neutral counterparts.

Table 1. The adsorption energy of N_2O (E_{ads}), the largest activate energies $E_{\text{a}}^{\text{max}}(N_2O)$ and $E_{\text{a}}^{\text{max}}(CO)$, and the desorption energies $E_{\text{des}}^{N_2}$ and $E_{\text{des}}^{CO_2}$ in the reaction pathway of the $Pt_lAu_m^-$ clusters. The dissociation energies (E_{dis}) of $Pt_lAu_m^-$ and Pt_lAu_m (shown in the parenthesis) clusters are also listed. All values are in units of eV.

Cluster	E_{ads}	$E_{\text{a}}^{\text{max}}(N_2O)$	$E_{\text{a}}^{\text{max}}(CO)$	$E_{\text{des}}^{N_2}$	$E_{\text{des}}^{CO_2}$	E_{dis}
Pt_4^-	1.30	0.35	0.57	1.32	1.28	2.97 (2.77)
Pt_3Au^-	1.51	0.44	0.51	1.46	1.69	2.65 (2.37)
$Pt_2Au_2^-$	1.54	0.40	0.11	1.47	0.95	2.30 (2.05)
$PtAu_3^-$	1.49	0.39	0.20	1.11	0.89	2.04 (1.77)

Figure 1 shows the most stable structures and their frontier molecular orbitals (FMOs) isosurfaces for CO, N_2O, $Pt_lAu_m^-$, and $[Pt_lAu_m(N_2O)]^-$ clusters. N_2O has a linear structure with $C_{\infty v}$ point symmetry. The bond lengths of N–N and N–O are 1.13 Å and 1.20 Å in this work, which are in very good agreement with the experimental results of 1.14 Å and 1.18 Å, respectively. The reduction of N_2O by CO in the absence of a catalyst has a high activation barrier of about 47.2 kcal/mol, and is exothermic by 87.0 kcal/mol.[9] So the binding of N_2O molecules on catalysts is considered as a necessary step for the consequent N_2O decomposition.

To find the most favorable geometries of the $[Pt_lAu_m(N_2O)]^-$ clusters, various possible binding sites of the molecule on the clusters and different relative orientations between the cluster and the molecule have been used as the initial geometries. The adsorption site of the molecule on the catalyst can be predicted with the frontier molecular orbital theory by observing the interaction between the highest occupied orbital (HOMO) and the lowest unoccupied molecule orbital (LUMO).[25]

We take Pt_4^- as an example to illustrate how it works. The Pt_4^- cluster has a rhombus structure as shown in Fig. 1. The HOMO and LUMO of Pt_4^- mainly locate at the Pt atom of the inner obtuse angle, while the HOMO and LUMO of the N_2O molecule mainly locate at the terminal N atom. When the N_2O

molecule is imported, the terminal N atom is bound to the Pt atom of the inner obtuse angle to constitute the $[Pt_4(N_2O)]^-$ cluster. Our DFT calculations confirm this result. Incidentally, with more Pt atoms replaced by Au atoms, the interaction between N_2O and the catalyst drastically modifies the structure of the cluster, as shown in Fig. 1 for Pt_3Au^-, $Pt_2Au_2^-$, and $PtAu_3^-$. It may be caused by the net charge transfer from the metal cluster to the N_2O molecule when the N_2O molecule is adsorbed on the $Pt_lAu_m^-$ cluster. For example, without adsorbing N_2O, the structure of $[PtAu_3]^-$ is a caped triangle; it changes to the rhombus structure when N_2O is adsorbed.

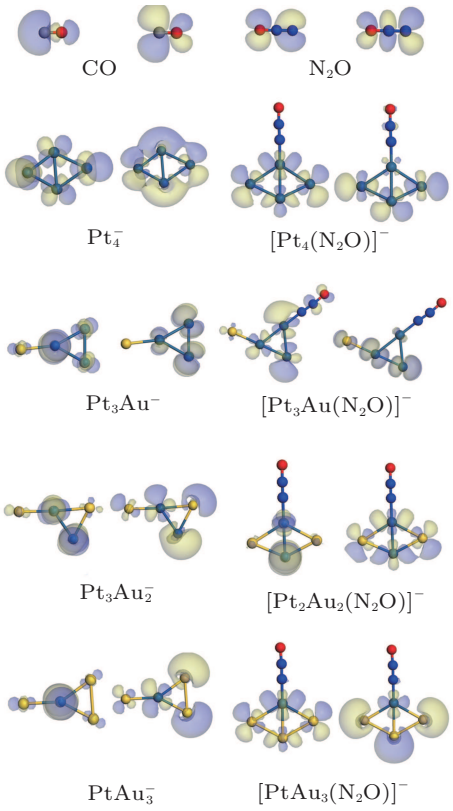


Fig. 1. (color online) Equilibrium structures and their FMOs isosurfaces for CO, N_2O, $Pt_lAu_m^-$, and $[Pt_lAu_m(N_2O)]^-$ clusters. The purple, yellow, grey, blue, and red spheres represent platinum, gold, carbon, nitrogen, and oxygen atoms, respectively.

When the N_2O molecule is adsorbed on the $Pt_lAu_m^-$ cluster, the N–O bond length of the N_2O molecule is significantly elongated compared to its gas-phase value (1.20 Å). Generally, the N–O bond length is around 1.24 Å for all four $Pt_lAu_m^-$ clusters. In our study, when N_2O is bound to the clusters, the calculated E_{ads} of N_2O on Pt site in Pt_3Au^-, $Pt_2Au_2^-$, $PtAu_3^-$ are 1.51 eV, 1.54 eV, and 1.49 eV (Table 1), respectively. These values are slightly larger than the corresponding adsorption energy on the Pt_4^- cluster (1.30 eV).

3.2. Reaction mechanism of N_2O with CO over $Pt_lAu_m^-$ cluster

Figure 2 represents the potential energy surface profiles for the reduction of N_2O by CO over the $Pt_lAu_m^-$ $(l+m=4)$ catalysts. The energies of the intermediates (IM), the transition states (TS), and the products are referred to the energy of the entrance (the free catalyst, one isolated N_2O molecule, and one isolated CO molecule). The catalytic reaction pathways over the $Pt_lAu_m^-$ clusters, with the intermediates and the transition states, are also shown in Fig. 2.

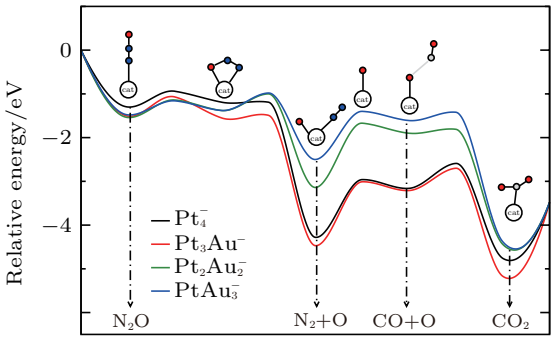


Fig. 2. (color online) The potential energy surfaces for reduction of N_2O by CO promoted by different $Pt_lAu_m^-$ clusters. The chemical formulas of the stable intermediates are shown at the bottom. The grey, blue, and red spheres represent carbon, nitrogen, and oxygen atoms, respectively. The cycles with "cat" denote the corresponding catalysts. The energy of the entrance is shifted to zero.

From Fig. 2, it can be concluded that the reaction processes over the $Pt_lAu_m^-$ catalysts are as follows. Firstly, a N_2O molecule is adsorbed on the optimized catalyst, forming a bridged intermediate state, and then the N–O bond is broken, a N_2 molecule forms and desorbs, which generates a corresponding oxidized cluster. Secondly, the oxygen atom of the oxidized cluster is seized by a CO molecule and one CO_2 molecule forms, then the CO_2 is desorbed by the catalyst.

We now illustrate the catalytic reaction over the Pt_3Au^- cluster. The N_2O molecule adsorbed on the Pt_3Au^- catalyst forms intermediate IM1 $[Pt_3Au(N_2O)]^-$, which locates at 1.51 eV below the entrance. The oxygen atom in the N_2O molecule is activated and the bond length of N–O is elongated (to 1.24 Å). Then the adsorbed N_2O bends toward an adjacent Pt atom and forms a bridged intermediate IM2 via transition state TS12 with a barrier of 0.44 eV. IM2 converts into IM3 and forms compound $[OPt_3AuN_2]^-$ via transition state TS23 with a barrier of 0.06 eV, in which the N–O bond is broken. This step is strongly exothermic (4.47 eV). After the N_2 is desorbed, the oxygen atom in the N_2O molecule is combined to the Pt_3Au^- cluster, forming IM4, which is an oxidized cluster. Now a CO molecule is imported to bind with the oxygen atom, forming the intermediate IM5, which locates at −3.21 eV below the entrance. IM5 converts to IM6 via transition state TS56 with a barrier of 0.51 eV. IM5 dissociates directly to the CO_2 molecule and the Pt_3Au^- cluster, indicating the accomplishment of the reaction.

As shown in Table 1, for the Pt_4^- cluster, $E_{des}^{N_2}$ (1.32 eV) is a little larger than E_{ads} (1.30 eV), at the same time, $E_{des}^{CO_2}$ (1.28 eV) is a little smaller than E_{ads} (1.30 eV). With one Pt

atom replaced by an Au atom in the Pt_4^- cluster, the desorption energy $E_{des}^{CO_2}$ (1.69 eV) is larger than E_{ads} (1.51 eV) for the Pt_3Au^- cluster, which indicates that the catalyst is degraded. However, with more Pt atoms replaced by Au atoms, the desorption energies $E_{des}^{N_2}$ and $E_{des}^{CO_2}$ both decrease remarkably. The E_{ads} is larger than the desorption energies $E_{des}^{N_2}$ and $E_{des}^{CO_2}$, meanwhile $E_{des}^{CO_2}$ is smaller than $E_{des}^{N_2}$, which means that the poisoning is overcome. From Table 1, we also find that, as the proportion of Au atoms in the $Pt_lAu_m^-$ clusters increases, the activate energy $E_a^{max}(N_2O)$ for the elementary reaction $N_2O \rightarrow N_2 + O$ decreases from 0.44 eV to 0.39 eV, and $E_a^{max}(CO)$ for the elementary reaction $CO + O \rightarrow CO_2$ decreases remarkably. It means that with more Pt atoms replaced by Au atoms, more N_2O molecules are dissociated and more CO molecules are oxidized. So the catalytic performance can be improved via the replacement of more Pt atoms by Au atoms in the negatively charged cluster $Pt_lAu_m^-$ cluster.

3.3. Electronic properties of the catalysts

The projected densities of states (PDOS) of *M* 5d (metal 5d) and N 2p orbits for $Pt_lAu_m^-$ (left panel) and $[Pt_lAu_m(N_2O)]^-$ (right panel) are shown in Fig. 3. The occupied *M* 5d band centers are also indicated by the black arrows. The occupation numbers of the 5d6s6p orbitals in each atom for the Pt_4^-, $PtAu_3^-$, $[Pt_4(N_2O)]^-$, and $[PtAu_3(N_2O)]^-$ clusters are shown in Table 2. Without the adsorption of N_2O to the $Pt_lAu_m^-$ clusters, there are some peaks in the PDOS of the *M* 5d over the Fermi level (as shown in the left panel of Fig. 3). When the N_2O molecule is adsorbed on the $Pt_lAu_m^-$ clusters, the peaks for the majority *M* 5d states disappear, as shown in the right panel of Fig. 3. At the same time, the PDOS of the N 2p emerges on both sides far away from the Fermi level. In Table 2, we also notice that the occupation number for the Pt(1) atom changes from $5d^{8.79}6s^{1.01}6p^{0.31}$ to $5d^{8.60}6s^{0.92}6p^{0.41}$ when the N_2O molecule is bound to the Pt(1) atom (Pt_4^- to $[Pt_4(N_2O)]^-$). For $Pt_lAu_m^-$ and $[Pt_lAu_m(N_2O)]^-$, we find that the changes of the occupation numbers on 5d6s6p for the Pt atom adsorbed with N atom are similar. These clues indicate that one of the unoccupied *M* 6p orbitals interacts with the lone electron pair (LEP) of N_2O to form the σ coordination bond, while the partial bonding 5d orbitals and the anti-bonding π^* orbital of N_2O form the back donation π coordination bond. The σ and π coordination bonds make the compound more stable, which leads to the larger E_{ads} for the $Pt_lAu_m^-$ clusters (as shown in Table 1). The larger E_{ads} will enhance the catalytic performance.

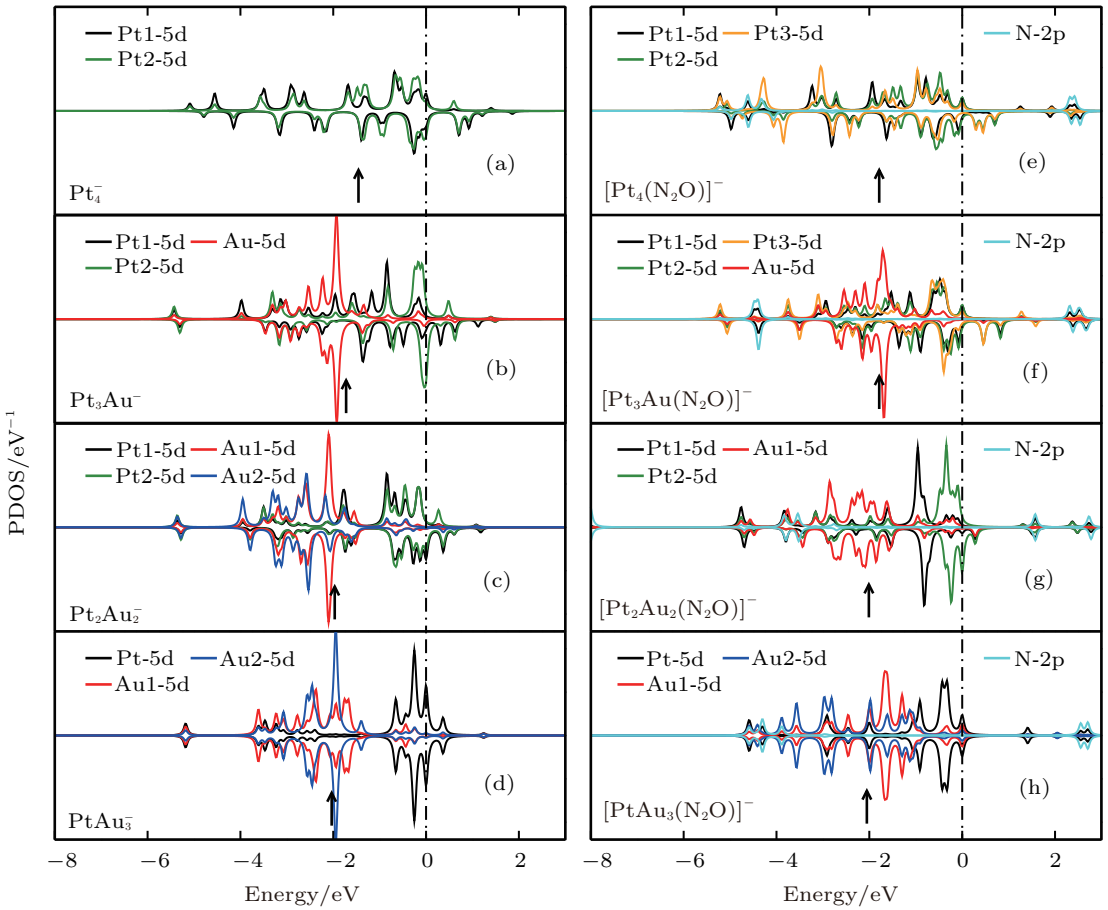


Fig. 3. (color online) The projected densities of states for the *M* 5d and N 2p of $Pt_lAu_m^-$ (left panel) and $[Pt_lAu_m(N_2O)]^-$ (right panel). The degenerate states are plotted once. The vertical dashed-dotted lines correspond to the Fermi level, and the black arrows are pointing to the occupied *M*-5d band center.

Table 2. The atomic charges and occupation numbers of the 5d6s6p orbital in each atom for the Pt_4^-, $PtAu_3^-$, $[Pt_4(N_2O)]^-$, and $[PtAu_3(N_2O)]^-$ clusters. The values in the parenthesis are the atom numbers in the clusters.

Cluster	Atom	Atomic charge	Orbital		
			5d	6s	6p
Pt_4^-	Pt(1)	–0.092	8.79	1.00	0.31
	Pt(2)	–0.408	8.96	1.30	0.15
	Pt(3)	–0.092	8.79	1.00	0.31
	Pt(4)	–0.408	8.96	1.30	0.15
$[Pt_4(N_2O)]^-$	Pt(1)	0.081	8.60	0.92	0.41
	Pt(2)	–0.341	8.91	1.28	0.16
	Pt(3)	–0.114	8.72	1.08	0.31
	Pt(4)	–0.342	8.91	1.28	0.16
$PtAu_3^-$	Au(1)	–0.433	9.78	1.58	0.08
	Pt(2)	–0.081	8.93	0.93	0.24
	Au(3)	–0.243	9.81	1.25	0.19
	Au(4)	–0.243	9.81	1.25	0.19
$[PtAu_3(N_2O)]^-$	Au(1)	–0.319	9.80	1.33	0.19
	Pt(2)	0.054	8.72	0.87	0.37
	Au(3)	–0.319	9.80	1.33	0.19
	Au(4)	–0.128	9.72	1.11	0.31

From the left panel of Fig. 3, it can be seen that, with increasing proportion of Au in the $Pt_lAu_m^-$ clusters, the width of PDOS for *M* 5d declines, and the PDOS of *M* 5d is concentrated on one area from (−5.5 eV, 1.0 eV) to (−3.8 eV, 0.2 eV), which means that the catalytic activity of more inner *M*-5d electron will be improved. At the same time, there is strong orbital hybridization between the Pt and Au atoms, which results in the down shift of the *M*-5d band center of the $Pt_lAu_m^-$ clusters away from the Fermi level. It is interesting to find that, as the *M*-5d band center of $Pt_lAu_m^-$ shifts down (shown in the left panel of Fig. 3), the largest activate energies for the elementary reaction $N_2O \rightarrow N_2 + O$ and the elementary reaction $CO + O \rightarrow CO_2$ are decreased remarkably (shown in Fig. 2 and Table 1), at the same time, the desorption energies $E_{des}^{N_2}$ and $E_{des}^{CO_2}$ in the reaction pathway (shown in Fig. 2 and Table 1) are reduced remarkably. This is consistent with the improved catalytic properties of $Pt_lAu_m^-$ with increasing proportion of Au in the bimetallic cluster. So the catalytic activity will be enhanced by the synergetic effect between Pt and Au atoms in bimetallic clusters $Pt_lAu_m^-$ compared to pure Pt_4^- or Au_4^-.

It is interesting to find that the reaction center is the Pt atom as shown in Fig. 1. When the N_2O molecule is adsorbed on the $Pt_lAu_m^-$ clusters, the terminal N atom is bound to the Pt atom. If the N_2O molecule is bound to the Au atom, the adsorption energy E_{ads} is very small, which means that the interaction between N_2O and the metal cluster is very weak, then the first step of the catalytic reaction cannot proceed. This is why Au_4^- shows little catalytic activity for the reaction of N_2O and CO. We also notice that the σ–π coordination bonds enhance the interaction between the metal cluster and N_2O, and result in a net charge transfer from the metal cluster to the N_2O molecule, which weakens the N–O bond in the N_2O molecule and results in longer N–O bond. Therefore, the N_2O molecule is bent to the metal cluster and the N–O bond is easily broken. So the Pt atom in the $Pt_lAu_m^-$ cluster is the reaction center, and all metal atoms act as electron donors.

4. Conclusion

The catalytic properties of $Pt_lAu_m^-$ ($l+m=4$) clusters for the removal of N_2O with CO are systematically investigated. The potential energy surfaces of the reaction are determined and characterized by first-principle calculations. We find that N_2O tends to adsorb on the Pt atom, and the dissociation energy of N_2O seems to be independent of its surroundings. With the increasing ratio of Au in the cluster, the activation energy for CO oxidation and desorption of the reaction products (N_2 and CO_2) can be significantly reduced. Compared to other $Pt_lAu_m^-$ clusters, the $PtAu_3^-$ bimetallic cluster exhibits better catalytic performance in the conversion of N_2O by CO to N_2 and CO_2.

References

[1] Ravishankara A R, Daniel J S and Portmann R W 2009 *Science* **326** 123
[2] Hamilton S M, Hopkins W S, Harding D J, Walsh T R, Haertelt M, Kerpal C, Gruene P, Meijer G, Fielicke A and Mackenzie S R 2011 *J. Phys. Chem. A* **115** 2489
[3] Chiodo S, Rondinelli F, Russo N and Toscano M 2008 *J. Chem. Theory Comput.* **4** 316
[4] Delabie A and Pierloot K 2002 *J. Phys. Chem. A* **106** 5679
[5] Wannakao S, Nongnual T, Khongpracha P, Maihom T and Limtrakul J 2012 *J. Phys. Chem. C* **116** 16992
[6] Blagojevic V, Orlova G and Bohme D K 2005 *J. Am. Chem. Soc* **127** 3545
[7] Ryan M F, Stoeckigt D and Schwarz H 1994 *J. Am. Chem. Soc* **116** 9565
[8] Michalak A, Witko M and Hermann K 1997 *J. Mol. Catal. A: Chemical* **119** 213
[9] Kappes M M and Staley R H 1981 *J. Am. Chem. Soc* **103** 1286
[10] Chen L L, Lu Q L and Luo Q Q 2010 *Acta Phys. Sin.* **59** 234 (in Chinese)
[11] Mao H P, Sheng Y and Wang H Y 2008 *Chin. Phys. B* **17** 2110
[12] Achatz U, Berg C, Joos S, Fox B S, Beyer M K, Niedner-Schatteburg G and Bondybey V E 2000 *Chem. Phys. Lett.* **320** 53
[13] Zhou M, Zhang A, Dai Z, Zhang C and Feng Y P 2010 *J. Chem. Phys.* **132** 194704
[14] Wang Y C, Wang Q Y, Geng Z Y, Si Y B, Zhang J H, Li H Z and Zhang Q L 2008 *Chem. Phys. Lett.* **460** 13
[15] Yamamoto H, Miyajima K and Yasuike T 2013 *J. Phys. Chem. A* **117** 12175
[16] Brönstrup M, Schröder D, Kretzschmar I, Schwarz H and Harvey J N 2001 *J. Am. Chem. Soc* **123** 142
[17] Balteanu I, Petru Balaj O, Beyer M K and Bondybey V E 2004 *Phys. Chem. Chem. Phys.* **6** 2910
[18] Siu C K, Reitmeier S J, Balteanu I, Bondybey V E and Beyer M K 2007 *Eur. Phys. J. D* **43** 189
[19] Wang F, Zhang D and Ding Y 2010 *J. Phys. Chem. C* **114** 14076
[20] Gao G P, Wei S H and Duan X M 2012 *J. Phys. Chem. C* **116** 24930
[21] Wang Y H, Zhu J L, Zhang J C, Song L F, Hu J Y, Ong S L and Ng W J 2006 *J. Power Sources* **155** 440
[22] Hammer B, Hansen L B and Nørskov J K 1999 *Phys. Rev. B* **59** 7413
[23] Delley B 1990 *J. Chem. Phys.* **92** 508
[24] Delley B 2000 *J. Chem. Phys.* **113** 7756
[25] Chretien S, Gordon M S and Metiu H 2004 *J. Chem. Phys.* **121** 3756